

Article

Long-Term Tree-Ring Response to Drought and Frost in Two *Pinus halepensis* Populations Growing under Contrasting Environmental Conditions in Peninsular Italy

Alfredo Di Filippo ^{1,*} , Michele Baliva ¹ , Michele Brunetti ² and Luca Di Fiore ¹ 

¹ DendroLab, Department of Agriculture and Forest Science (DAFNE), Università della Tuscia, 01100 Viterbo VT, Italy; m.baliva@unitus.it (M.B.); difiore@unitus.it (L.D.F.)

² CNR-ISAC, 40129 Bologna BO, Italy; m.brunetti@isac.cnr.it

* Correspondence: difilippo@unitus.it

Abstract: *Pinus halepensis* dominates coastal to mountain areas throughout the Mediterranean Basin. Its growth plasticity, based on polycyclic shoot formation and dynamic cambial activity, and tolerance to extreme drought and exceptional frosts, allows it to colonize a vast array of environments. We used tree-rings from codominant pines to compare lifespan, growth rates, age and size distribution in a typical coastal (i.e., prolonged drought, occasional low-intensity fires) vs. inland hilly (i.e., moister conditions, recurrent frosts) population. BAI trends, growth-limiting climate factors and tree-ring anatomical anomalies were analyzed considering the differences in climate and phenology obtained from multispectral satellite images. The species maximum lifespan was 100–125 years. Mortality was mainly due to fire on the coast, or heart-rot in the inland site. Populations differed in productivity, which was maintained over time despite recent warming. Site conditions affected the growing season dynamics, the control over ring formation by summer drought vs. winter cold and the frequency of anatomical anomalies. Recurrent frost rings, associated with temperatures below -10°C , occurred only at the inland site. *Pinus halepensis* confirmed its remarkable growth plasticity to diverse and variable environmental conditions. Its ability to survive extreme events and sustain productivity confirmed its adaptability to climate change in coastal areas as well as on Mediterranean mountains.

Keywords: Aleppo pine; forest; BAI; tree-rings; lifespan; phenotypic traits; intra-annual density fluctuations; climate-change



Citation: Di Filippo, A.; Baliva, M.; Brunetti, M.; Di Fiore, L. Long-Term Tree-Ring Response to Drought and Frost in Two *Pinus halepensis* Populations Growing under Contrasting Environmental Conditions in Peninsular Italy. *Forests* **2021**, *12*, 305. <https://doi.org/10.3390/f12030305>

Academic Editor: Rosana López Rodríguez

Received: 31 January 2021

Accepted: 2 March 2021

Published: 6 March 2021

Publisher's Note: MDPI stays neutral with regard to jurisdictional claims in published maps and institutional affiliations.



Copyright: © 2021 by the authors. Licensee MDPI, Basel, Switzerland. This article is an open access article distributed under the terms and conditions of the Creative Commons Attribution (CC BY) license (<https://creativecommons.org/licenses/by/4.0/>).

1. Introduction

The Mediterranean Basin is an important biodiversity hotspot particularly vulnerable to climate change impacts [1]. In the last decades, progressive drying up and temperature increases have been reported [2], making future scenarios for vegetation dynamics not optimistic [3]. Furthermore, extreme events such as heat waves or dry spells, and even frost, have been reported to increase in frequency and severity [4].

Aleppo pine (*Pinus halepensis* Mill.) is the most widely distributed pine in the Mediterranean Region. Its natural distribution range over the Mediterranean Basin extends from North Africa (Morocco, Algeria) to Syria and from Portugal to Greece [5]. It is often replaced by *Pinus brutia* Ten. in the eastern part of the Mediterranean Basin. It is generally found at low elevation, from sea level to 600 m a.s.l. in northern populations, but it reaches 1000 m a.s.l. in Southern Spain and 1700 m a.s.l. in North Africa. Aleppo pine is a pioneer species and a key component of Mediterranean forest dynamics in many areas. Light demanding and thermophilous, its exceptional plasticity allows it to colonize and grow in very hot and dry sites and on every type of non-hydromorphic soil [5]. Aleppo pine disrespects high humidity, frost and snow, but is able to survive and grow in a range of different environments, from meso-mediterranean to semi-arid climate spanning annual temperature in the range of $10\text{--}20^{\circ}\text{C}$ and precipitation 300–1000+ mm [6]. The ability to

adjust its physiology and growing season to variable drought severity implies intrinsic eco-physiological adjustments [7,8]. In addition, the polycyclism of Aleppo pine represents a key trait for the adaptation to the high variability of the Mediterranean climate, whose long and severe summer droughts divide the growing season into two parts [9]. The number and rates of flushes vary with the prevailing climatic conditions in the growing season, with shoot formation ending in autumn with the short photoperiod and cold temperatures [10]. Nonetheless, it may not be uncommon that mild conditions in late fall stimulate a new flush and growth continues until the next spring.

The absence of a true dormancy in the cambium of *Pinus halepensis* has been reported in warm Mediterranean sites (e.g., coastal areas in Eastern Spain), where xylogenesis continues with varying rates throughout the year, whereas in cooler sites (e.g., Slovenia) it can stop for 1 to 3 months during winter [11]. In addition, the cambial activity in *Pinus halepensis* can slow down and stop during summer drought and resumes in late summer-autumn once moisture availability increases (e.g., [12]), then stop again when winter temperatures drop. As a consequence, its radial growth often presents a bimodal pattern (e.g., [11,13]). Large scale dendroecological studies [6] have shown that tree-ring width is generally promoted by precipitation in many months of the year. Especially May emerges as a key month, probably for the importance of spring shoot development for the overall tree performance [10]. Temperature is generally negatively correlated to growth rates during the central months of the year, but warmth has positive effects in the previous winter and in November of the year of ring formation [6].

In the last years, the research on the growth plasticity of Aleppo pine has received new stimulus with the definition and identification of the so-called Intra Annual Density Fluctuations (IADFs). IADFs occur when unusual conditions alter the normal radial growth (e.g., latewood-like cells within the earlywood and vice versa). They are classified according to their anatomical structure and relative position within tree-rings, and can be useful to define influences on radial growth caused by climatic fluctuations [14]. Summer drought and autumn precipitation have been reported as the main drivers of IADFs in *Pinus halepensis* [15]. Under severe stress conditions in extreme sites it may omit the xylem ring formation, an additional demonstration of its plasticity [16]. In general, the use of pointer years in dendroecology has often provided interesting insights on the biology of tree species and their response to extreme events [17]. Wood anatomical anomalies, such as fire scars or light rings, carry environmental clues that have greatly contributed to reconstructing the ecological history of large territories (e.g., fire history, insect outbreaks). Among the many features potentially available, those approaches allowing to evaluate cold adaptation in tree species and reconstruct the recurrence of frost events have been explored either using the “blue-rings” approach [18] or the so-called “frost rings”, i.e., layers of deformed or collapsed vessels and traumatic parenchyma cells corresponding to the occurrence of extreme cold events in periods of cambial activity [19]. Frost rings, sometimes becoming cracks in the core in correspondence of the parenchyma layer [20], may represent interesting long-term ecological archives if long tree-ring series are available.

In this study, we used tree-ring variability, wood anatomical anomalies, and remotely sensed phenology of two *Pinus halepensis* populations growing in the Italian Peninsula under contrasting ecological conditions (inland with cold and moist winter vs. coastal with pronounced summer drought and milder winter) with the aim to characterize the plasticity of the species and its response to climate change. In particular, we: (1) described the main biological features of the two populations in terms of lifespan, size, growth rates; (2) characterized and compared the ecology of the species in such different growth conditions (3) identified the main climatic events that affected the growth history of the two populations and their response to climate variability.

2. Materials and Methods

2.1. Study Sites

The sampled sites were located in the central (Val Serra) and southern (Monte Barone) part of the Italian Peninsula (Figure 1). In Val Serra, pine populations grew near the city of Terni, at an elevation varying between 490 and 730 m a.s.l. on North-West to South-West aspects. The mean slope is c. 27°, but variable along the mountain side. The climate is cold in winter, frost risk interests several spring and autumn months, and summer drought is limited. These ecosystems have been ascribed to moist pine forests types, but growing on shallow soils [21]. Our study area fell within two vegetation types: at low elevation, pine-dominated stands with *Cupressus sempervirens* L. on dry marly arenaceous soils; at higher elevation, Aleppo pine is facilitated as a standard after logging in a mixed coppice dominated by *Quercus ilex*, on limestone soils. We found no direct information on the forest's history. At least part of it has been interested in the past by afforestation operations, i.e., presence of stone walls, to enhance its role as a protection forest.

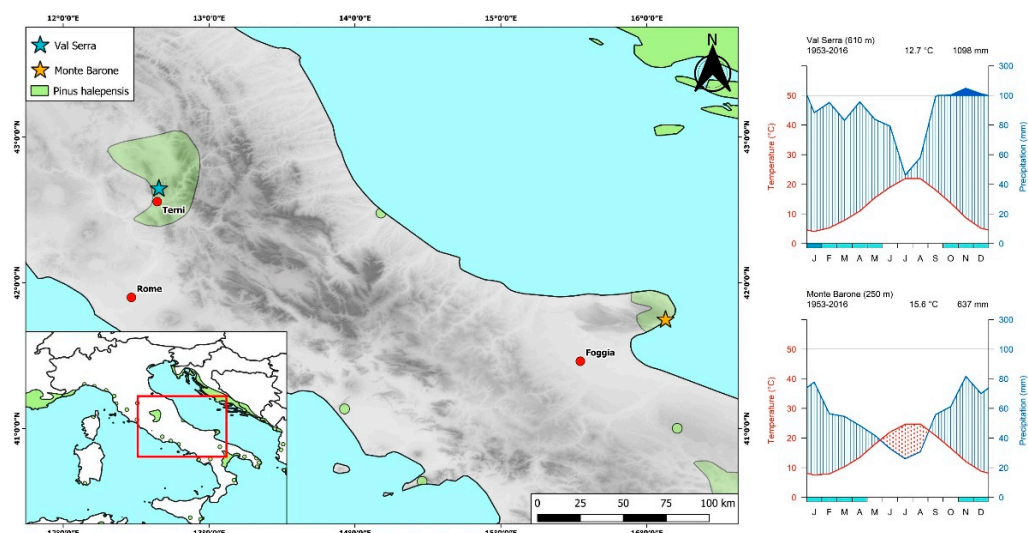


Figure 1. Study sites position in relation to *Pinus halepensis* distribution range [22] and their corresponding climatic diagrams (according to Walter and Lieth).

Monte Barone is a Natural Biogenetic State Reserve of 124 ha established in 1977 and managed by Carabinieri Reparto Biodiversità, falling in the Municipality of Mattinata within the Gargano National Park. The Gargano Promontory hosts some of the best-preserved natural populations of *Pinus halepensis*. The climate is hot and dry, with a marked summer drought. The stand structure is uneven-aged, stratified after recurrent surface low-intensity fires occurred in past decades (0.2 ha in 8 September 2008; 3 ha in 29 June 2010; 0.2 ha in 19 August 2010; data provided by Col. Claudio Angeloro, Reparto Biodiversità Foresta Umbra, Carabinieri Forestali). Pines dominate the forests, where they may be associated with holm oak (*Quercus ilex* L.) and downy oak (*Quercus pubescens* Willd.) and an understory rich in shrub species typical of the Mediterranean scrub. The elevation ranges from 200 to 300 m a.s.l. with a North/North-East aspect and average slope c. 13° (Table 1), with particularly rugged topography. The soils are of the brown type, moderately deep.

Table 1. Geographical features of the two study sites.

Site	Samples	Latitude (°)	Longitude (°)	Elevation Range (m a.s.l.)	Slope (°)	Aspect
Val Serra	35	42.6448	12.6565	490–730	26.8	SW
Monte Barone	23	41.7450	16.1303	200–300	12.9	NE

2.2. Tree-Ring Data Collection and Analysis

Using a dendroecological approach, the sampled trees were cored at 1.3 m using increment borers and an associated set of metadata was collected (DBH; GPS coordinates and elevation; Table 2). A total of 58 trees were sampled, 23 at Monte Barone (in 2019) and 35 at Val Serra (in 2016) taking one sample per tree on the uphill side of the stem. In the laboratory, all increment cores were mounted, sanded, and surfaced with scalpels. Tree-ring widths were measured to the nearest 0.01 mm using a Computer Controlled Tree-Ring Measure Device (CCTRMD) interfaced with the software CATRAS. Earlywood and latewood were measured separately, subjectively distinguished according to the sharp transition between large thin-walled earlywood cells and the small thick-walled latewood cells, generally demarcated by a line of resin ducts. Synchronized and crossdated tree-ring series were kept for dendroecological investigations.

Table 2. Tree-ring sampling and dendrochronological features of the two study sites. Basal area increment (BAI) values and mean earlywood and latewood widths are referred to the common 50-year period (1967–2016). EPS: Expressed population signal.

Site	N Samples	DBH ¹ (cm)	Age ¹ (yr)	BAI ¹ (cm ² /yr)	Earlywood Width ¹ (mm/yr)	Latewood Width ¹ (mm/yr)	EPS > 0.85	N Trees ²
Val Serra	35	44 ± 10 (25–62)	79 ± 24 (35–122)	16.1 ± 3.2 (7.0–42.1)	1.13 ± 0.70 (0.10–7.26)	0.39 ± 0.24 (0.02–3.12)	1920–2016	10
Monte Barone	23	45 ± 4 (37–52)	64 ± 12 (43–97)	23.7 ± 6.6 (12.0–35.8)	1.79 ± 0.69 (0.15–9.68)	0.56 ± 0.22 (0.06–4.53)	1952–2019	10

¹ Mean values and standard deviation, range in parentheses. ² Minimum number of trees included in the mean BAI chronologies in the period with EPS > 0.85.

Crossdated cores were visually examined under a stereomicroscope for the presence of Inter Annual Density Fluctuation (IADFs), i.e., “a layer of cells within a tree-ring identified by different shape, size and wall thickness” and other pointer years [14], in particular, Frost Rings (FR), Non-Dormant Cambium (NDC, i.e., non-abrupt transition between latewood of the previous year and earlywood of the next year), Resin Canals into the Earlywood (*ewRCs*). IADFs were classified considering their position within the latewood, tagged as IADF *L** by merging the categories IADF *L+* and IADFs *L* described by Novak et al. [23]. IADFs and frost rings were easily distinguished in annual tree-rings and allowed to investigate intrannual growth response due to changes in climatic conditions.

For each type of pointer years (*L**, *FR*, *NDC*, *ewRC*) we calculated the overall frequency within each population and the annual frequency. To understand if tree age and position may affect the occurrence of frost rings, the most represented events were analyzed in more detail.

Tree-ring width time series were used to calculate basal area increment (BAI; a proxy for annual biomass production [24]) using the *dplR* package [25]. Individual raw BAI series were averaged to produce a raw BAI chronology to explore productivity trends. We analyzed the relationships between the individual BAI and tree age or size. All calculations were performed using the R software [26].

2.3. The Climate-Growth Relationships

Tree-ring width, earlywood and latewood series were standardized by fitting a cubic smoothing spline with a 50-year period and a 50% frequency response to preserve high-frequency, while minimizing age- and size-related trends. Standardized series were then averaged to form a ring-width, earlywood or latewood standardized chronology, validated according to the expressed population signal (EPS > 0.85) and prewhitened by an autoregressive model selected according to the Akaike Information Criterion [27]. Bootstrap correlation functions were calculated between each prewhitened site chronology and the corresponding monthly climatic variables (maximum and minimum temperature, precipitation) spanning a 20-month window, from December of the current growth year to

May of the previous year. Monthly precipitation and minimum/maximum temperature data were estimated by applying a weighted linear regression to a high-density network of meteorological stations (details in [28]). Weights were assigned to stations according to their similarity in geographic parameters (distance, elevation, slope steepness and orientation, distance from the sea) with those of the study sites.

2.4. Satellite Data Analysis

Sentinel-2 images are provided by the European Space Agency (ESA) at a maximum spatial resolution of 10 m and time resolution of 5 days, when the satellites Sentinel-2A and -2B are combined together. We chose all Sentinel-2 pixels close to the GPS points of the dendroecological sampling and corresponding to homogenous forest sectors (i.e., dense and continuous canopy cover). To enhance the homogeneity of the remote sensing sampling, we discarded areas characterized by frequent shadows in winter due to their slope and aspect (e.g., North to East).

Twenty-four and nineteen pixels were retained at Monte Barone and Val Serra, respectively. Sentinel-2 surface reflectance images (Level 2A), atmospherically and topographically corrected using the Sen2Cor processor [29], were collected on the Google Earth Engine platform [30], accessed from R using the package “rgee” [31]. Starting from the first complete year of level 2A directly provided by ESA (2018) until 2020, only the scenes with a cloud presence less than 20% were retained. The remaining low-quality data (medium and high probability of clouds, their shadows, and thin cirri) were masked using the Sen2Cor scene classification [29]. The dates with more than 50% masked pixels were not considered in the analyses to reduce the uncertainty associated with the reduced replication (186 scenes for Monte Barone, 75 for Val Serra). Spectral bands were combined to calculate the Enhanced Vegetation Index (EVI, [32]) using the same coefficients developed for MODIS:

$$EVI = 2.5 * \frac{NIR - RED}{(NIR + 6 * RED - 7.5 * BLUE + 1)} \quad (1)$$

NIR, RED, and BLUE represent the reflectance in the near-infrared, red and blue spectral regions, respectively. EVI is a better proxy of forest vegetation activity and biomass than the more commonly used Normalized Difference Vegetation Index (NDVI), reducing the background influence and avoiding index saturation over high biomass areas [33].

The observations of the available 3 years (2018–2020) were temporally merged to create a single 1-year time series for each Sentinel-2 pixel. To remove the remaining variability connected to noise factors (e.g., low-quality observations not masked by the scene classification) and improve the reliability of the raw data [34], time series were smoothed using a LOESS (Locally Estimated Scatterplot Smoothing) filter. The flexibility of the filter was chosen using the cross-validation method [35]. To represent the average phenology of each site, we calculated the median and standard error of each pixel for each day of the year.

3. Results

3.1. Tree Age, Size, and Growth Rates

The analysis of codominant Aleppo pines showed reduced size variability both in Val Serra and Monte Barone, with a mean diameter of 44 ± 10 cm and 45 ± 4 cm, respectively. However, the maximum size was 10 cm larger in Val Serra than in Monte Barone. Moreover, the mean and maximum age were higher at Val Serra (79 ± 24 years, maximum 122 years) than Monte Barone (64 ± 12 years, maximum 97 years) expanding over a rather wide age distribution in both sites (Table 2). The age structure of codominant trees showed a rather continuous recruitment, with the absence of strongly synchronized regeneration peaks, which may suggest that continuous natural dynamics have structured both populations, especially at Monte Barone where there was no significant age-DBH relationship (Figure 2).

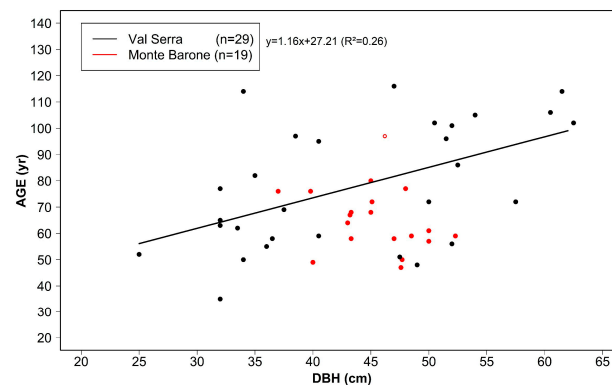


Figure 2. The relationship between diameter at breast height (DBH) and age (number of years, yr), modelled by linear regression for Val Serra (black; equation in the plot, $p < 0.01$) and Monte Barone (red; non-significant). Only samples with pith were used (number of replicates in the legend). The empty red circle indicates the oldest tree in Monte Barone, where the pith was missing.

Maximum growth rates reached $35\text{--}45\text{ cm}^2\text{ yr}^{-1}$ in both sites, at a comparable age and size (50–60 years, 50 cm). Especially at Monte Barone, the increase in productivity with size was much steeper (Figure 3b). When the overall period of analysis (1967–2016) was divided into two halves (1967–1991 and 1992–2016, the latter one characterized by warmer-drier climatic conditions) the relationships became weaker in the recent period (1992–2016; Figure S1a, right), or not significant in the older one (1967–1991; Figure S1b, right). When considering age as a predictor of BAI, relations were rarely significant, and older trees showed lower growth rates (Figure 3, Figure S1a,b).

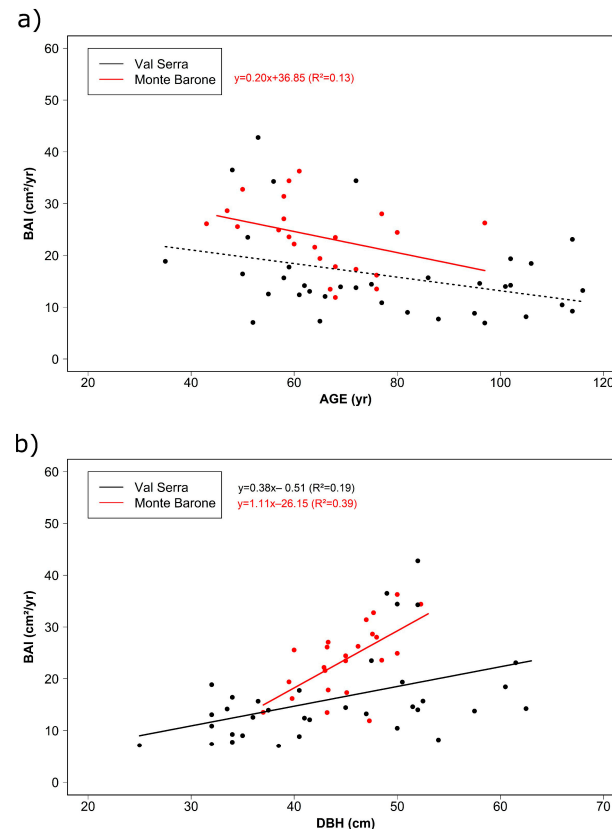


Figure 3. Linear regression between BAI (1967–2016) vs. trees age (a) and DBH (b) for Val Serra (black) and Monte Barone (red). Continuous lines represent a significant regression ($p < 0.05$), whose equations are reported in the plot with colour corresponding to the site.

Monte Barone showed higher values than Val Serra both for mean correlation with master chronology (0.68 ± 0.12 vs. 0.58 ± 0.16) and mean sensitivity (0.34 ± 0.03 vs. 0.26 ± 0.04), which respectively indicated a stronger common signal and higher year-to-year growth variability. Raw BAI chronology at Monte Barone showed a constant increasing trend culminating in the mid-1970s, followed by a stable mean productivity with important intra-annual variability (Figure 4). The lowest productivity minimum occurred between 1989 and 1990. At Val Serra, BAI had less variability and showed a slight decrease starting since the mid-1970s, with a minimum in 1985. Over the last 40 years, both populations showed no significant long-term productivity trend in response to the climatic drying up of the last decades.

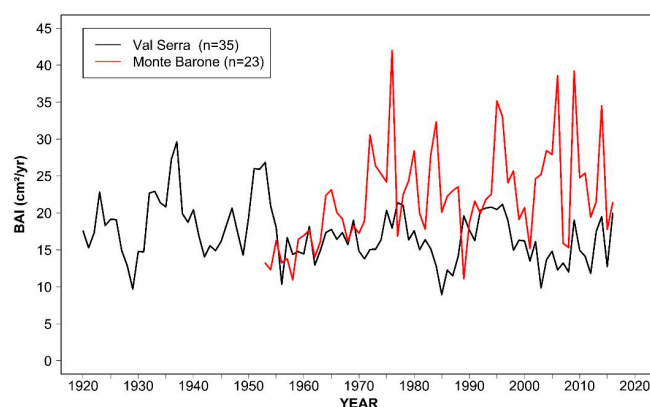


Figure 4. Comparison between mean BAI chronologies of the two study sites. Chronologies validated according to their EPS: Val Serra, 1920–2016; Monte Barone, 1953–2019.

Tree-rings showed different earlywood and latewood average widths (Table 2, Figure 5). Regarding earlywood, both sites showed a decreasing trend since the mid-1970s, but Val Serra had overall lower values and showed a less steep decreasing trend. Latewood width chronologies were stable and similar among the sites, with more pronounced interannual fluctuations at Monte Barone.

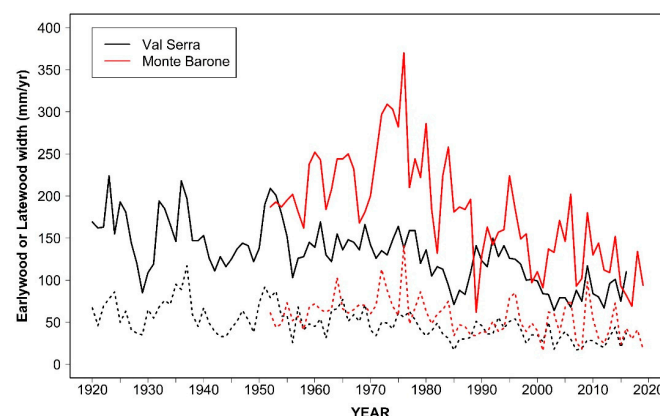


Figure 5. Comparison between earlywood (solid line) and latewood (dashed line) width chronologies for the two study sites. Chronologies were validated according to their EPS.

3.2. Climate-Growth Relationships

The prewhitened site ring-width chronologies of Val Serra and Monte Barone were scarcely correlated (Pearson's $r = 0.12$), linked to different climatic drivers influencing the tree growth. Growth variability is controlled by summer drought and winter temperature at both sites, but with different coefficients and months involved (Table 3). The summer response was significant in June and August in the colder site (Val Serra), while especially August assumes a greater importance in the warmer one (Monte Barone). The winter cold

affects mainly Val Serra, but pines in Monte Barone prefer a low temperature in spring probably to avoid the late frost impact in this metabolically active period. In the year of ring formation, a warm December stimulates growth in both sites, while warmth in December before the growing season affects the two sites in an opposite way: negatively in the cold one (Val Serra), to avoid damage connected to frost; positively in the warm one (Monte Barone) to stimulate the continuation of cambial activity through winter. April precipitation gains significance only in the warm Monte Barone, probably in connection with early phases of shoot development. The presence of previous summer signals, i.e., positive effects of drought, are important only in the cold site and may be connected to cone abortion and their positive effect on wood growth.

Table 3. Bootstrap correlation functions calculated between the prewhitened tree-ring width chronologies of Val Serra and Monte Barone and monthly climatic data (time span: 1953–2016). Blue/red values indicate a significant positive/negative correlation ($p < 0.05$).

	Year Preceding Growth												Year of Growth											
	MAY	JUN	JUL	AUG	SEP	OCT	NOV	DEC	JAN	FEB	MAR	APR	MAY	JUN	JUL	AUG	SEP	OCT	NOV	DEC				
VAL SERRA																								
P	0.10	−0.03	−0.14	−0.30	−0.06	0.13	−0.05	0.08	−0.11	−0.09	−0.13	0.05	0.10	0.29	0.21	0.24	0.18	0.06	−0.05	0.09				
Tmax	0.05	0.08	0.34	0.36	−0.02	0.02	−0.21	−0.14	0.05	0.28	0.27	0.20	−0.05	−0.22	−0.19	−0.15	−0.13	−0.01	0.23	0.09				
Tmin	0.03	0.13	0.30	0.30	0.02	0.10	−0.12	−0.30	−0.03	0.19	0.18	0.24	0.04	−0.07	−0.07	−0.05	−0.04	0.05	0.14	0.21				
MONT BARONE																								
P	−0.07	−0.09	−0.08	0.08	−0.07	−0.07	0.20	0.16	0.25	0.06	0.07	0.24	0.17	0.25	0.30	0.46	0.10	0.13	−0.18	−0.01				
Tmax	0.16	0.05	0.05	0.02	0.05	−0.10	0.00	0.09	−0.09	−0.07	−0.27	−0.20	−0.09	−0.09	−0.20	−0.41	−0.27	−0.11	0.06	0.17				
Tmin	0.09	0.10	0.14	0.10	0.08	−0.15	0.12	0.22	0.09	0.04	−0.21	0.00	−0.08	−0.05	−0.05	−0.31	−0.11	−0.12	−0.04	0.23				

P, monthly precipitation; Tmax, monthly maximum temperature; Tmin, monthly minimum temperature.

Earlywood width was mainly affected by February–March temperatures of the current year, but with opposite effects in the two sites (Table 4). In the colder Val Serra, winter warmth stimulated earlywood formation, while in the warmer Monte Barone it is inversely correlated to March temperature, possibly in relation to late frost impacts on early onsets of physiological activity. Drought in June–July was key to discriminate between earlywood and latewood in the colder Val Serra (i.e., June was important for earlywood, July, August, and September for latewood). In the warmer Monte Barone, the onset of latewood can be traced back already to drought in June. Latewood formation responds to drought until September in Val Serra or October in Monte Barone. Latewood formation is strongly promoted by warm temperature in December, but only in the cold site.

Table 4. Bootstrap correlation function coefficients calculated between the prewhitened earlywood (a) and latewood (b) width chronologies of Val Serra and Monte Barone and monthly climatic data (time span: 1953–2016). Blue/red values indicate a positive/negative correlation ($p < 0.05$). In grey: Important months in determining the formation of earlywood vs. latewood.

	Year Preceding Growth												Year of Growth											
	MAY	JUN	JUL	AUG	SEP	OCT	NOV	DEC	JAN	FEB	MAR	APR	MAY	JUN	JUL	AUG	SEP	OCT	NOV	DEC				
VAL SERRA																								
(a)																								
P	0.08	0.00	−0.13	−0.12	0.06	0.02	−0.04	0.05	−0.09	−0.14	−0.14	0.06	0.11	0.33	0.06	0.07	0.00	0.11	−0.10	−0.05				
Tmax	−0.02	0.07	0.27	0.22	−0.09	0.01	−0.14	−0.05	0.15	0.37	0.29	0.11	−0.09	−0.26	−0.20	−0.04	0.02	−0.08	0.08	0.01				
Tmin	−0.01	0.16	0.25	0.19	0.03	0.11	−0.09	−0.16	0.12	0.29	0.20	0.15	0.07	−0.06	−0.13	0.04	0.05	0.03	−0.05	0.05				
(b)																								
P	0.15	0.05	−0.08	−0.27	−0.09	0.08	−0.01	0.03	−0.07	−0.01	−0.17	0.00	0.03	0.11	0.38	0.49	0.27	−0.07	−0.03	0.19				
Tmax	0.05	−0.11	0.19	0.33	−0.08	0.04	−0.26	−0.22	−0.13	0.22	0.24	0.08	−0.10	−0.09	−0.30	−0.43	−0.34	0.06	0.25	0.21				
Tmin	0.11	−0.04	0.18	0.30	−0.06	0.06	−0.20	−0.30	−0.19	0.17	0.08	0.08	0.00	−0.02	−0.08	−0.26	−0.11	0.11	0.22	0.44				
MONT BARONE																								
(a)																								
P	−0.15	−0.07	−0.05	0.09	−0.06	−0.01	0.20	0.13	0.23	0.16	0.10	0.26	0.18	0.19	0.09	0.26	−0.10	−0.01	−0.06	−0.03				
Tmax	0.22	0.03	0.03	0.00	0.04	−0.16	0.08	0.09	−0.09	−0.13	−0.34	−0.21	−0.17	−0.16	−0.08	−0.22	−0.05	0.01	0.02	0.08				
Tmin	0.08	0.11	0.09	0.03	0.09	−0.17	0.18	0.19	0.04	−0.02	−0.24	−0.04	−0.13	−0.09	−0.03	−0.20	−0.01	−0.03	−0.08	0.12				
(b)																								
P	−0.01	−0.04	0.01	0.18	0.05	−0.04	0.09	0.08	0.18	0.08	0.11	0.08	0.03	0.25	0.35	0.48	0.33	0.27	−0.21	0.08				
Tmax	0.08	−0.02	0.05	−0.07	−0.05	−0.06	0.01	0.02	−0.09	−0.01	−0.27	−0.10	0.11	0	−0.31	−0.41	−0.39	−0.32	0.15	0.11				
Tmin	0.02	0	0.10	0	0.01	−0.15	0	0.19	0.10	0.13	−0.19	0.03	0.10	0.07	−0.11	0.30	−0.13	−0.21	0.05	0.20				

P, monthly precipitation; Tmax, monthly maximum temperature; Tmin, monthly minimum temperature.

3.3. Satellite Data Analysis

Smoothed EVI values were characterized by low temporal variation during the study period (2018–2020; Figure 6a). Both sites had a similar average pattern, but a different variability and vegetation index values. Compared to Val Serra, Monte Barone showed higher EVI values, especially during the last part of spring, and higher inter-pixel variability, especially in winter when smoothed EVI values ranged approximately 0.15.

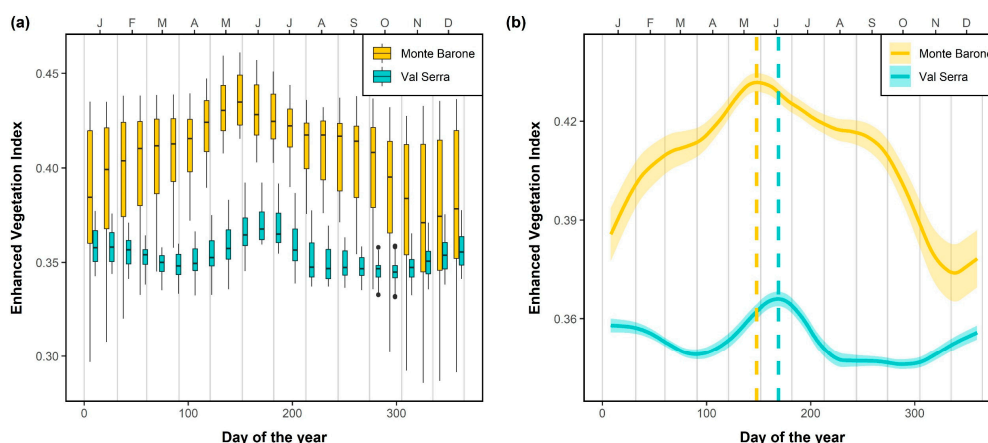


Figure 6. (a) Smoothed enhanced vegetation index (EVI) values for all the Sentinel-2 pixels summarized by a boxplot for each site and period (16 days). (b) LOESS (Locally Estimated Scatterplot Smoothing) curve of median EVI of all pixels (\pm standard error) for each site.

Maximum EVI values were obtained between May and June (Figure 6b), earlier and with a more pronounced peak at the warmer site (Monte Barone). The colder Val Serra showed sustained vegetation activity during the whole June, Monte Barone showed a faster after-peak decline. EVI decreased for both sites throughout July and, around mid-August, it stabilized at low levels in Val Serra, while the warmer Monte Barone showed a second lower peak in activity protracted until early October, after which it fell to minimum values.

3.4. Pointer Years and Frost Events

A total of 4,194 tree-rings were analyzed on cores from the two sites (Val Serra, 2715; Monte Barone, 1479) where we found a total of 224 pointer years, 114 in Val Serra and 110 in Monte Barone, distributed among four different types (L^* ; $ewRC$; NDC ; FR) (Figure 7a). IADF L^* was the most represented type in both sites (Figure 7), with a higher frequency and the maximum in the last three decades (Val Serra: 2004; Monte Barone: 2009). NDC was rarely found in both sites, occurring more frequently only in a few years (1954 and 1984 in Val Serra; 1989 in Monte Barone). In addition, $ewRC$ was the second most frequent type in the warmer Monte Barone, not found in the colder Val Serra. Frost rings occurred only in Val Serra (Figure 7b). We found a total of 29 tree-rings with distorted tissue damaged by frost, with the highest frequency in 1956 (16%), 1963 (21%), 1985 (29%), as a consequence of cold events in the first months of the year (January or February; Table S1). Frost rings were identified especially in trees at higher elevation, but with significant differences only in 1985 (Figure 8). In this year, trees growing above c. 550 m a.s.l. were more susceptible to frost. Age did not influence the occurrence of frost rings, both young (even with a few years) and old trees were interested (no significant age difference found).

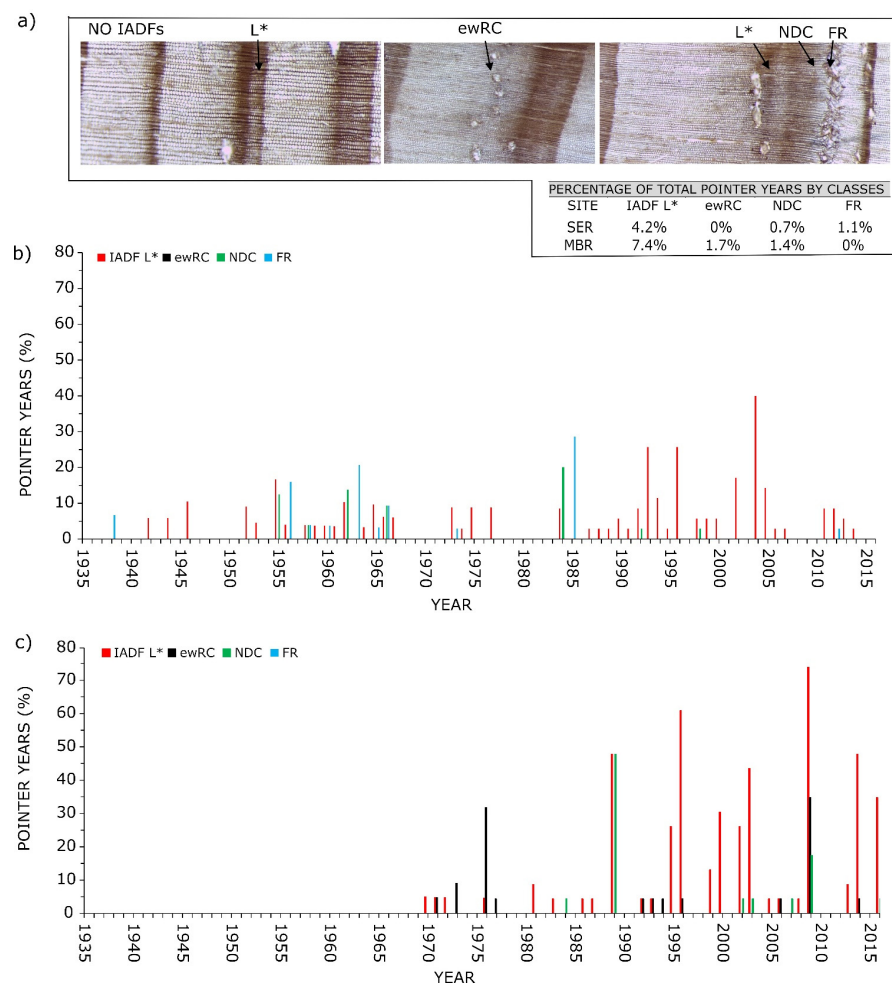


Figure 7. (a) Different types of pointer years detected and their percentage of occurrence. *L**: Inter-annual density fluctuation in latewood; *ewRC*: Resins canals in the earlywood; *NDC*: Non-dormant cambium, i.e., continuous shift from latewood to earlywood; *FR*: Frost ring characterized by distorted xylem tissue or callous tissue. (b) Val Serra pointer year frequency. (c) Monte Barone pointer year frequency. Data plotted since 1935, since 1937 was the first year with a pointer ring.

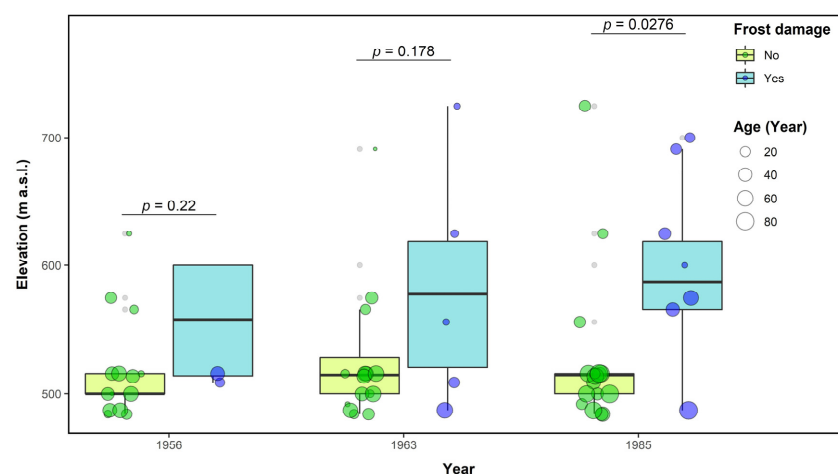


Figure 8. Elevation covered by the three most important frost events. Boxplots were referred to all the available trees grouped by year, highlighting elevation differences between damaged and undamaged trees (p -values from a non-paired t -test). Coloured points refer to trees with pith, their size proportional to age.

4. Discussion

The analysis of the two selected *Pinus halepensis* populations confirmed the high plasticity of the species and its ability to occupy largely different climatic conditions, from extremely dry to cold-moist winter conditions in the Mediterranean Basin [5]. The two sites well represent the contrasting environmental conditions experienced by the species in the North side of the Mediterranean Basin, where it can dominate coastal forests and, occasionally, sub-mediterranean, cooler areas. In the cooler inland site (Val Serra), in addition to the lower average temperature, annual precipitation sums up to almost double that in the coastal-southern site, and frost risk is present in several months (also in autumn and spring). The two populations differed substantially in maximum size, productivity, phenology, and climate signals controlling earlywood and latewood growth. Alongside the lack of correlation between their growth chronologies, these differences testify both the spectrum of ecological conditions covered by Aleppo pine across its range and the effectiveness of using it for dendroclimatic studies [6]. A further dimension of the study is represented by within-site differences among trees indicating that, besides the existing common pattern of year-to-year variation, important micro-environmental effects in *Pinus halepensis* populations are due to their open structure or soil features [5].

Pinus halepensis crown phenology inferred from EVI at the two sites showed comparable seasonal patterns, but earlier effects of drought and prolonged activity in the second part of the year at the warmer site. EVI steeply increased in April–May and peaked in late May–June. The onset of activity corresponded to the rapid shoot growth rate in spring reported for the species [10]. However, in the warmer Monte Barone, the EVI peak was anticipated by c. 20 days and declined earlier, but kept a second activity peak in August to early October. Due to its colder environmental conditions, Val Serra showed a longer duration of peak activity in June, but no signs of continuation through late summer–autumn. Our EVI phenology showed a similar amplitude, but different patterns compared to the NDVI phenology from lower resolution sensors in Spain [36] and Greece (investigating *Pinus halepensis* and *Pinus pinea* populations, [37]), which showed a winter peak in the vegetation index followed by a second peak in spring. Conversely, our EVI profiles were more similar to the NDVI dynamics of the mixed *Pinus pinea* and *Pinus pinaster* stand in Central Italy [38]. Compared to the broadleaf species, the phenology from vegetation indices should be used with more caution in evergreen conifers, since their lower intra-annual range makes it difficult to isolate the vegetation activity from other noise factors [39]. Despite the topographic correction, the high winter EVI variability could be connected, especially on N-NE aspects, to topographic effects [40].

In both sites, the species did not show exceptionally high longevity, i.e., the oldest sampled trees have c. 100 years (Monte Barone) or 125 years (Val Serra). Such lifespans are in line with what was found in many parts of the Mediterranean, but remain lower than the 150–200 years reported for *Pinus halepensis* longevity [6]. Novak [23] reported a maximum lifespan of 215 years from the cross-dated tree-ring series in Spain. In Val Serra, where slower growth rates could be a promoting factor of a long lifespan [41–43], the maximum age did not surpass 125 years. Interestingly, the same maximum age emerged in a previous (2004) sampling from the same forest: in 2016, we found several trees close to the same maximum age, but no one older. Moreover, in most of the largest trees, we observed the presence of heart-rotting fungi (Figure S2), such as *Porodaedalea pini* (Brot.) Murrill 1905, suggesting a potential limit in cool-wet environments connected to pathogens. The occurrence of wood scars associated with recurrent frosts (see below) could represent a potential entrance for infection: in this cool-moist valley protected by wind, where fire is a minor disturbance, heart-rot may be a chief agent of density-independent mortality. In Monte Barone, instead, recurrent fires (generally low-intensity ones within the site, but reaching higher intensity on nearby coasts) may represent a factor hampering the development of very old trees. This is testified by the limited size realized by pines here and the presence of several large trees with fire scars (Figure S2). It is remarkable, however,

to have spots in the Reserve able to preserve old trees (c. 100 years old), important to sustain the natural dynamics of this unique stand in Italy.

The average tree productivity was higher in the warmer site, despite longer and harsher summer droughts, highlighting the important role of a long growing season for *Pinus halepensis* [6]. In the cooler Val Serra, although site conditions allow the survival of larger trees, growth rates remained lower. BAI at the warmer Monte Barone was similar to what was reported in Southern Spain populations [44]. In both cases, and with a similar variation to Southern Spain, individual tree productivity showed a remarkable variability, possibly connected to the uneven-aged and open structure of both stands, as well as the geomorphologic within-stand differences (ridge vs. slope, rocky vs. forest soils). Within each Aleppo pine population, the highest growth rates were observed in trees with DBH around 50 cm and age below 50–60 years old. While no sampled tree exceeded 50 cm in Monte Barone, larger trees (DBH > 50 cm) in the moister site (Val Serra) showed lower growth rates. Growth rates are expected to increase with tree size [45] but, especially in drought-prone areas, a larger size may correspond to the higher exposure to hydraulic failure (e.g., [46]). Another explanation may be found in the higher exposure of larger trees to canopy damage by frost or other disturbances. In the warmer site (Monte Barone), the lack of very large trees may be attributed to the recurrence of anthropogenic surface fires: in nearby *Pinus halepensis* populations growing at a similar elevation, but in more protected conditions (e.g., “Pineta Marsini”), the species can show higher DBH.

Tree productivity has remained relatively stable in both sites since the 70s, with the warmer Monte Barone keeping higher BAI. Studies analyzing growth trends in *P. halepensis* are rare. In Southern Spain, Linares et al. [44] found a similar behaviour in the last decades (70s-), and explained it with the ability of the species to keep lower water costs under increasing long-term drought. The stability of BAI trends demonstrated the high plasticity of Aleppo pine in terms of tolerance to warm-dry periods [11] in comparison to other tree species, characterized by increasing summer drought impacts in the same period (e.g., [47]). However, under extremely dry conditions, even Aleppo pine may show substantial growth declines [48]. Tree-ring formation may be omitted in exceptionally dry years in extremely dry environments [16], but we found only one missing ring among thousands demonstrating that our sites are not yet close to the dry limit of this species. In any case, the growing season actual evapotranspiration remains the main driver of growth dynamics [49], being *P. halepensis* well adapted to the scarcity of water resources [7,8]. While the cooler Val Serra showed less sensitive growth rates, Monte Barone had frequent spikes in latewood width with higher interannual variability. A longer growing season under warmer climatic conditions may compensate for the longer drought stress [11]. Interestingly, earlywood width at both sites stabilized in the last 20 years (possibly in connection with the so-called “climate hiatus”, [50]) while, interestingly, latewood widths were often comparable. The warmer site (Monte Barone) showed substantially higher peaks after 2000, possibly connected to an extension of the growing season under the warm autumn conditions, which frequently occurred in the last two decades [11].

Growth variability was controlled by summer drought and winter temperature at both sites, in line with the presence of double stress throughout the year and the species' ability to resume the cambium activity [6]. However, the dynamics were differently modulated by the two populations according to the site temperature: cambial dynamics may stop for 1 to 3 months in winter, and slow down or stop during summer drought [11]. Ring-width at the colder and moister Val Serra was cold-limited in the previous winter, but more responsive throughout summer and favoured by warmth in current winter. A warm December could stimulate growth continuation especially in cold sites, and have lower importance in warmer ones [11]. The warmer Monte Barone did not show a cold limitation to the onset of the growing season, or for its prolongation. It may be limited, instead, if a warmer spring exposes the shoot development to late frosts. In addition, it was interested by an earlier onset of drought effects on latewood formation (June), with a key role of August in determining the overall ring-width. Its latewood responded to

drought until October (September in Val Serra). The Aleppo pine growth biology allows it to stop cell formation during dry phases and quickly recover it when water becomes available, so that the summer drought duration and severity have a key role in determining growth dynamics [10]. Overall, site differences in xylogenesis dynamics reflected the differences in phenology and were in line with what was expected from warm dry vs. cooler temperature populations [11]. De Luis et al. [6] reported similar considerations by studying the tree-ring response of the species across its range: The winter response changed from positive to negative moving from mesic to drier sites, and the response to precipitation disappeared as the summer drought severity increases, with trees entering a quiescent and nonreactive state.

An emblematic trait describing *Pinus halepensis* growth plasticity is its ability to form IADFs (4%–7% measured rings in our case), generally connected to prolonged latewood formation with earlywood-like cells, related to the recovery of growth after the summer drought [15]. IADFs showed increasing frequencies since the 90s at both sites, demonstrating their strict connection with warming and summer drought conditions [14]. Both sites may show a continuous shift from latewood to earlywood in years when cambium appeared as non-dormant, indicating growth continuation throughout winter even in the colder site [11]. In warm sites, cambium of *P. halepensis* may show enlarging cells in winter, and latewood tracheids formed in the previous growing season continued secondary wall formation and lignification through winter until the next calendar year [23]. The formation of new xylem may thus overlap with the final development of the terminal cells of the previous ring. This is an advantage, especially in coastal warm areas, such as Monte Barone, where extreme frosts are unlikely (no temperature colder than $-10\text{ }^{\circ}\text{C}$ since 1900; Table S1). The continuation of cambial activity may instead become a problem in frost-prone internal areas: five frost events were recorded into rings of the colder Val Serra, coinciding with some of the lowest temperatures registered in Italy since the beginning of the XX century (January or February daily minimum temperature dropped below $-10\text{ }^{\circ}\text{C}$ in 1938, 1956, 1963, 1985, 2012). Several of these exceptional years were also highlighted by Galli [51] as growth minima in *Pinus pinea* in Ravenna, on the Adriatic coast of Italy. Freezing temperatures when the cambium is active trigger the formation of tree-rings characterized by traumatic tissues (i.e., frost rings) in both angiosperms and conifers. Frost rings, made of unusual axial parenchyma cells or tracheids with an irregular structure, appear in the annual secondary xylem as a layer of crushed, irregular cells. They represent the most extreme form of wood anatomical imprints left by extreme temperature, formed with freezing conditions below species-specific thresholds [52]. In *Pinus halepensis*, we found that at least one day below $-10\text{ }^{\circ}\text{C}$ is enough to affect ring formation. The existence of non injured rings in years with comparable temperature drops hinted at the additional role played by previous autumn-winter weather conditions on predisposing trees to frost damage. Several studies have observed this anomaly in tree-rings produced by a young cambium [52], but in Val Serra we found this phenomenon in individuals of every age and size. Among all frost events, what happened in Italy in January 1985 deserves a special mention: most of the first half of the month was well below $0\text{ }^{\circ}\text{C}$, and the minimum temperature remained below $-10\text{ }^{\circ}\text{C}$ for 6 days (absolute minimum, 12 January: $-13.3\text{ }^{\circ}\text{C}$; Table S1). This year expands the tolerance limit of the species, known to tolerate winter temperatures as low as $-12\text{ }^{\circ}\text{C}$ [53]. The 1985 event, indeed, remained impressed in climatological and agricultural archives: most olive trees died in orchards in inland areas, and large rivers (e.g., the Arno in Florence) or the Venice Lagoon froze [54].

The frost events registered in *Pinus halepensis* demonstrated the plasticity of this thermophilous species to survive recurrent frosts, a trait that distinguishes the Umbria provenances [53]. It could also provide interesting clues to interpret the ecological history of the species in inland areas of Central Italy, where its naturalness has been questioned [55]. In Val Serra, frost effects were pronounced especially above 550–600 m a.s.l., where old trees were absent. Given the age distribution of pines, it is plausible that its expansion above that elevation has been favoured by the warmer temperatures only in the last decades. The

ability of the species to resist extreme frosts may also suggest that its presence in internal areas could have occurred naturally, even during colder climatic phases (e.g., the Little Ice Age, LIA), at least on south-western aspects below 500 m a.s.l. (minimum elevation in the surroundings reaches c. 100 m a.s.l.). In nearby areas (Rieti Basin), long-term palynological studies have demonstrated the continuous presence of *Pinus* pollen during the alternating climatic phases (e.g., Warm Medieval Epoch, LIA) of the last 2000 years [56]. Among the pine species potentially interesting Central Italy, *P. halepensis* certainly represents one of the best candidates for colonizing the area of Terni (Val Nerina).

The adaptability of *Pinus halepensis* to a vast range of ecological conditions in the Mediterranean Basin can greatly rely on the growth plasticity of its cambium. Nonetheless, in colder areas, its inability to stop in winter may convert the advantage to dangerous exposure to risk. Even in this case, Aleppo pine demonstrated its tolerance of exceptionally low temperatures: all pines with frost rings were in good health at the time of sampling. On the Gargano Promontory, oppositely, the pines at Monte Barone showed an interesting increase in latewood density fluctuations stimulated by warming in recent decades. Only here we found resin ducts in earlywood, of probable traumatic origin and related to early drought occurrences or other ecological factors (e.g., insects). Dendroclimatic studies including pointer years, either IADFs or anatomical features, demonstrated a great potential to describe forest ecological history and tree response to climate change.

Supplementary Materials: The following are available online at <https://www.mdpi.com/1999-4907/12/3/305/s1>. Figure S1: Relationship between average basal area increment (BAI) vs. trees age (left) or diameter at breast height (DBH; right), modelled by a simple linear regression ($p < 0.05$), for the periods 1992–2016 (a), 1967–1991 (b); Table S1: Absolute minimum annual temperatures and number of days in years with temperature falling below -10°C or -5°C in Val Serra and Monte Barone, respectively. Correspondence between years with low temperatures and frost rings are highlighted; Figure S2: Example of Aleppo pine trees and their cause of death: Fire scar at Monte Barone (left, photograph by Alfredo Di Filippo), stem decay fungus at Val Serra (right, photograph by Edoardo Esposito).

Author Contributions: Conceptualization, A.D.F.; methodology and formal analysis, A.D.F., L.D.F., and M.B. (Michele Baliva); climatic data, M.B. (Michele Brunetti); writing—review and editing, A.D.F., L.D.F., and M.B. (Michele Baliva). All authors have read and agreed to the published version of the manuscript.

Funding: The research on Monte Barone was conducted with funding by Parco Nazionale del Gargano.

Acknowledgments: We greatly thank Colonnello Claudio Angeloro (Carabinieri-Reparto Biodiversità Foresta Umbra) for providing historical data on the Monte Barone State Reserve and the support to field sampling logistics, and Brigadiere Capo Vincenzo Fasanella and Luogotenente Antonio Bisanzio (Carabinieri Forestali) for the cooperation in the field campaign. We thank the B.Sc. student Edoardo Esposito for his collaboration in field and laboratory operations on Val Serra cores.

Conflicts of Interest: The authors declare no conflict of interest.

References

1. Cuttelod, A.; García, N.; Malak, D.A.; Temple, H.; Katariya, V. The Mediterranean: A biodiversity hotspot under threat. In *Wildlife in a Changing World—An Analysis of the 2008 IUCN Red List of Threatened Species*; IUCN: Gland, Switzerland, 2008.
2. Hoerling, M.; Eischeid, J.; Perlwitz, J.; Quan, X.; Zhang, T.; Pegen, P. On the increased frequency of mediterranean drought. *J. Clim.* **2012**, *25*, 2146–2161. [CrossRef]
3. Lionello, P.; Scarascia, L. The relation between climate change in the Mediterranean region and global warming. *Reg. Environ. Chang.* **2018**, *18*, 1481–1493. [CrossRef]
4. Sánchez, E.; Gallardo, C.; Gaertner, M.A.; Arribas, A.; Castro, M. Future climate extreme events in the Mediterranean simulated by a regional climate model: A first approach. *Glob. Planet. Chang.* **2004**, *44*, 163–180. [CrossRef]
5. Chambel, M.R.; Climent, J.; Pichot, C.; Ducci, F. Mediterranean Pines (*Pinus halepensis* Mill. and *brutia* Ten.). In *Forest Tree Breeding in Europe*; Springer: Dordrecht, The Netherlands, 2013; ISBN 978-94-007-6145-2.
6. De Luis, M.; Čufar, K.; Di Filippo, A.; Novak, K.; Papadopoulos, A.; Piovesan, G.; Rathgeber, C.B.K.; Raventós, J.; Saz, M.A.; Smith, K.T. Plasticity in dendroclimatic response across the distribution range of Aleppo pine (*Pinus halepensis*). *PLoS ONE* **2013**, *8*, e83550. [CrossRef] [PubMed]

7. Borghetti, M.; Cinnirella, S.; Magnani, F.; Saracino, A. Impact of long-term drought on xylem embolism and growth in *Pinus halepensis* Mill. *Trees Struct. Funct.* **1998**, *12*, 187–195. [\[CrossRef\]](#)
8. Klein, T. Eco-Physiology of Water Use in *Pinus halepensis*: From Leaf to Forest Scale. Ph.D. Thesis, Scientific Council of the Weizmann Institute of Science, Rehovot, Israel, 2012.
9. Hover, A.; Buissart, F.; Caraglio, Y.; Heinz, C.; Pailler, F.; Ramel, M.; Vennetier, M.; Prévosto, B.; Sabatier, S. Growth phenology in *Pinus halepensis* Mill.: Apical shoot bud content and shoot elongation. *Ann. For. Sci.* **2017**, *74*. [\[CrossRef\]](#)
10. Pardos, M.; Climent, J.; Gil, L.; Pardos, J.A. Shoot growth components and flowering phenology in grafted *Pinus halepensis* Mill. *Trees Struct. Funct.* **2003**, *17*, 442–450. [\[CrossRef\]](#)
11. Prislán, P.; Gričar, J.; de Luis, M.; Novak, K.; Del Castillo, E.M.; Schmitt, U.; Koch, G.; Štrus, J.; Mrak, P.; Žnidarič, M.T.; et al. Annual cambial rhythm in *Pinus halepensis* and *Pinus sylvestris* as indicator for climate adaptation. *Front. Plant. Sci.* **2016**, *7*, 1923. [\[CrossRef\]](#)
12. Baquedano, F.J.; Valladares, F.; Castillo, F.J. Phenotypic plasticity blurs ecotypic divergence in the response of *Quercus coccifera* and *Pinus halepensis* to water stress. *Eur. J. For. Res.* **2008**, *127*, 495–506. [\[CrossRef\]](#)
13. Camarero, J.J.; Olano, J.M.; Parras, A. Plastic bimodal xylogenesis in conifers from continental Mediterranean climates. *New Phytol.* **2010**, *185*, 471–480. [\[CrossRef\]](#) [\[PubMed\]](#)
14. Campelo, F.; Nabais, C.; Freitas, H.; Gutiérrez, E. Climatic significance of tree-ring width and intra-annual density fluctuations in *Pinus pinea* from a dry Mediterranean area in Portugal. *Ann. For. Sci.* **2007**, *64*, 229–238. [\[CrossRef\]](#)
15. Zalloni, E.; de Luis, M.; Campelo, F.; Novak, K.; De Micco, V.; Di Filippo, A.; Vieira, J.; Nabais, C.; Rozas, V.; Battipaglia, G. Climatic signals from intra-annual density fluctuation frequency in mediterranean pines at a regional scale. *Front. Plant. Sci.* **2016**, *7*, 579. [\[CrossRef\]](#) [\[PubMed\]](#)
16. Novak, K.; de Luis, M.; Saz, M.A.; Longares, L.A.; Serrano-Notivol, R.; Raventós, J.; Čufar, K.; Gričar, J.; Di Filippo, A.; Piovesan, G.; et al. Missing rings in *Pinus halepensis*—The missing link to relate the tree-ring record to extreme climatic events. *Front. Plant. Sci.* **2016**, *7*, 727. [\[CrossRef\]](#) [\[PubMed\]](#)
17. Fritts, H.C.; Swetnam, T.W. Dendroecology: A tool for evaluating variations in past and present forest environments. *Adv. Ecol. Res.* **1989**, *19*, 111–188.
18. Piermattei, A.; Crivellaro, A.; Carrer, M.; Urbinati, C. The “blue ring”: Anatomy and formation hypothesis of a new tree-ring anomaly in conifers. *Trees Struct. Funct.* **2015**, *29*, 613–620. [\[CrossRef\]](#)
19. Montwé, D.; Isaac-Renton, M.; Hamann, A.; Spiecker, H. Cold adaptation recorded in tree rings highlights risks associated with climate change and assisted migration. *Nat. Commun.* **2018**, *9*, 1–7. [\[CrossRef\]](#)
20. Barinov, V.V.; Mygland, V.S.; Taynik, A.V.; Oydupa, O.C.; Vaganov, E.A. Extreme climatic events in the Republic of Tuva according to tree-ring analysis. *Contemp. Probl. Ecol.* **2015**, *8*, 414–422. [\[CrossRef\]](#)
21. Pedrotti, F. Notizia di ricerche fitosociologiche sulle pinete a Pino d'Aleppo della valle del serra (Terni). *Mitt. Ostalp. Pflanz. Arb.* **1967**, *7*, 139–142.
22. Caudullo, G.; Welk, E.; San-Miguel-Ayanz, J. Chorological maps for the main European woody species. *Data Br.* **2017**, *12*, 662–666. [\[CrossRef\]](#)
23. Novak, K.; Čufar, K.; De Luis, M.; Sánchez, M.A.S.; Raventós, J. Age, climate and intra-annual density fluctuations in *Pinus halepensis* in Spain. *IAWA J.* **2013**, *34*, 459–474. [\[CrossRef\]](#)
24. Di Filippo, A.; Biondi, F.; Maugeri, M.; Schirone, B.; Piovesan, G. Bioclimate and growth history affect beech lifespan in the Italian Alps and Apennines. *Glob. Chang. Biol.* **2012**, *18*, 960–972. [\[CrossRef\]](#)
25. Bunn, A.; Korpela, M.; Biondi, F.; Campelo, F.; Mérian, P.; Qeadan, F.; Zang, C.; Buras, A.; Cecile, J.; Mudelsee, M.; et al. (Eds.) Package “dplR”, Version 1.7.1. In *Dendrochronology Program Library in R*; R Foundation: Vienna, Austria, 2015.
26. R Core Team. *R: A Language and Environment for Statistical Computing*; R Foundation for Statistical Computing: Vienna, Austria, 2020.
27. Di Filippo, A.; Biondi, F.; Čufar, K.; De Luis, M.; Grabner, M.; Maugeri, M.; Presutti Saba, E.; Schirone, B.; Piovesan, G. Bioclimatology of beech (*Fagus sylvatica* L.) in the Eastern Alps: Spatial and altitudinal climatic signals identified through a tree-ring network. *J. Biogeogr.* **2007**, *34*, 1873–1892. [\[CrossRef\]](#)
28. Brunetti, M.; Maugeri, M.; Nanni, T.; Simolo, C.; Spinoni, J. High-resolution temperature climatology for Italy: Interpolation method intercomparison. *Int. J. Climatol.* **2014**, *34*, 1278–1296. [\[CrossRef\]](#)
29. Louis, J.; Debaecker, V.; Pflug, B.; Main-Knorn, M.; Bieniarz, J.; Mueller-Wilm, U.; Cadau, E.; Gascon, F. Sentinel-2 SEN2COR: L2A processor for users. *Eur. Sp. Agency (Spec. Publ.) ESA SP* **2016**, *SP-740*, 9–13.
30. Gorelick, N.; Hancher, M.; Dixon, M.; Ilyushchenko, S.; Thau, D.; Moore, R. Google Earth Engine: Planetary-scale geospatial analysis for everyone. *Remote Sens. Environ.* **2017**, *202*, 18–27. [\[CrossRef\]](#)
31. Aybar, C.; Wu, Q.; Bautista, L.; Yali, R.; Barja, A. rgee: An R package for interacting with Google Earth Engine. *J. Open Source Softw.* **2020**, *5*, 2272. [\[CrossRef\]](#)
32. Huete, A.R.; Liu, H.Q.; Batchily, K.; van Leeuwen, W. A comparison of vegetation indices over a global set of TM images for EOS-MODIS. *Remote Sens. Environ.* **1997**, *59*, 440–451. [\[CrossRef\]](#)
33. Huete, A.; Didan, K.; Miura, T.; Rodriguez, E.P.; Gao, X.; Ferreira, L.G. Overview of the radiometric and biophysical performance of the MODIS vegetation indices. *Remote Sens. Environ.* **2002**, *83*, 195–213. [\[CrossRef\]](#)

34. Cai, Z.; Jönsson, P.; Jin, H.; Eklundh, L. Performance of smoothing methods for reconstructing NDVI time-series and estimating vegetation phenology from MODIS data. *Remote Sens.* **2017**, *9*, 1271. [CrossRef]
35. Golub, G.H.; Heath, M.; Wahba, G. Generalized cross-validation as a method for choosing a good ridge parameter. *Technometrics* **1979**, *21*, 215–223. [CrossRef]
36. Aragones, D.; Rodriguez-Galiano, V.F.; Caparros-Santiago, J.A.; Navarro-Cerrillo, R.M. Could land surface phenology be used to discriminate Mediterranean pine species? *Int. J. Appl. Earth Obs. Geoinf.* **2019**, *78*, 281–294. [CrossRef]
37. Karamihalaki, M.; Stagakis, S.; Sykioti, O.; Kyparissis, A.; Parcharidis, I. Monitoring drought effects on mediterranean conifer forests using spot-vegetation NDVI and NDWI timeseries. *Eur. Sp. Agency (Spec. Publ.) ESA SP* **2016**, *SP-740*, 603.
38. Maselli, F. Monitoring forest conditions in a protected Mediterranean coastal area by the analysis of multiyear NDVI data. *Remote Sens. Environ.* **2004**, *89*, 423–433. [CrossRef]
39. Zeng, L.; Wardlow, B.D.; Xiang, D.; Hu, S.; Li, D. A review of vegetation phenological metrics extraction using time-series, multispectral satellite data. *Remote Sens. Environ.* **2020**, *237*, 111511. [CrossRef]
40. Chen, R.; Yin, G.; Liu, G.; Li, J.; Verger, A. Evaluation and normalization of topographic effects on vegetation indices. *Remote Sens.* **2020**, *12*, 2290. [CrossRef]
41. Di Filippo, A.; Pederson, N.; Baliva, M.; Brunetti, M.; Dinella, A.; Kitamura, K.; Knapp, H.D.; Schirone, B.; Piovesan, G. The longevity of broadleaf deciduous trees in Northern Hemisphere temperate forests: Insights from tree-ring series. *Front. Ecol. Evol.* **2015**, *3*. [CrossRef]
42. Piovesan, G.; Biondi, F.; Baliva, M.; Dinella, A.; Di Fiore, L.; Marchiano, V.; Presutti Saba, E.; De Vivo, G.; Schettino, A.; Di Filippo, A. Tree growth patterns associated with extreme longevity: Implications for the ecology and conservation of primeval trees in Mediterranean mountains. *Anthropocene* **2019**, *26*, 100199. [CrossRef]
43. Brienen, R.J.W.; Caldwell, L.; Duchesne, L.; Voelker, S.; Barichivich, J.; Baliva, M.; Ceccantini, G.; Di Filippo, A.; Helama, S.; Locosselli, G.M.; et al. Forest carbon sink neutralized by pervasive growth-lifespan trade-offs. *Nat. Commun.* **2020**, *11*, 4241. [CrossRef]
44. Linares, J.C.; Delgado-Huertas, A.; Carreira, J.A. Climatic trends and different drought adaptive capacity and vulnerability in a mixed *Abies pinsapo*-*Pinus halepensis* forest. *Clim. Chang.* **2011**, *105*, 67–90. [CrossRef]
45. Stephenson, N.L.; Das, A.J.; Condit, R.; Russo, S.E.; Baker, P.J.; Beckman, N.G.; Coomes, D.A.; Lines, E.R.; Morris, W.K.; Rüger, N.; et al. Rate of tree carbon accumulation increases continuously with tree size. *Nature* **2014**, *507*, 90–93. [CrossRef] [PubMed]
46. Rowland, L.; Da Costa, A.C.L.; Galbraith, D.R.; Oliveira, R.S.; Binks, O.J.; Oliveira, A.A.R.; Pullen, A.M.; Doughty, C.E.; Metcalfe, D.B.; Vasconcelos, S.S.; et al. Death from drought in tropical forests is triggered by hydraulics not carbon starvation. *Nature* **2015**, *528*, 119–122. [CrossRef] [PubMed]
47. Piovesan, G.; Biondi, F.; Di Filippo, A.; Alessandrini, A.; Maugeri, M. Drought-driven growth reduction in old beech (*Fagus sylvatica* L.) forests of the central Apennines, Italy. *Glob. Chang. Biol.* **2008**, *14*, 1265–1281. [CrossRef]
48. Camarero, J.J.; Gazol, A.; Sangüesa-Barreda, G.; Oliva, J.; Vicente-Serrano, S.M. To die or not to die: Early warnings of tree dieback in response to a severe drought. *J. Ecol.* **2015**, *103*, 44–57. [CrossRef]
49. Rathgeber, C.B.K.; Misson, L.; Nicault, A.; Guiot, J. Bioclimatic model of tree radial growth: Application to the French Mediterranean Aleppo pine forests. *Trees Struct. Funct.* **2005**, *19*, 162–176. [CrossRef]
50. Trenberth, K.E.; Fasullo, J.T. An apparent hiatus in global warming? *Earth's Future* **2013**, *1*, 19–32. [CrossRef]
51. Galli, M.; Guadalupi, M.; Nanni, T.; Ruggiero, L.; Zuanni, F. Ravenna pine trees as monitors of winter severity in N-E Italy. *Theor. Appl. Climatol.* **1992**, *45*, 217–224. [CrossRef]
52. Hadad, M.; Tardif, J.C.; Conciatori, F.; Waito, J.; Westwood, A. Climate and atmospheric circulation related to frost-ring formation in *Picea mariana* trees from the Boreal Plains, interior North America. *Weather Clim. Extrem.* **2020**, *29*, 100264. [CrossRef]
53. Calamassi, R.; Paoletti, E.; Strati, S. Frost hardening and resistance in three Aleppo pine (*Pinus halepensis* Mill.) provenances. *Isr. J. Plant. Sci.* **2001**, *49*, 179–186. [CrossRef]
54. Camuffo, D.; Bertolin, C.; Craievich, A.; Granziero, R.; Enzi, S. When the Lagoon was frozen over in Venice from A.D. 604 to 2012: Evidence from written documentary sources, visual arts and instrumental readings. *Méditerranée. Rev. Géographique Des Pays Méditerranéens/J. Mediterr. Geogr.* **2017**. Available online: <https://journals.openedition.org/mediterranee/7983> (accessed on 4 March 2021).
55. Pignatti, S. *I Boschi d'Italia. Sinecologia e Biodiversità*; UTET: Torino, Italy, 1998.
56. Mensing, S.; Tunno, I.; Cifani, G.; Passigli, S.; Noble, P.; Archer, C.; Piovesan, G. Human and climatically induced environmental change in the Mediterranean during the Medieval Climate Anomaly and Little Ice Age: A case from central Italy. *Anthropocene* **2016**, *15*, 49–59. [CrossRef]